


Two-channel anomalous Hall effect in SrRuO₃Graham Kimbell ¹, Paul M. Sass ², Bart Woltjes ¹, Eun Kyo Ko,^{3,4} Tae Won Noh ^{3,4},
Weida Wu ² and Jason W. A. Robinson ^{1,*}¹*Department of Materials Science & Metallurgy, University of Cambridge, Cambridge CB3 0FS, United Kingdom*²*Department of Physics and Astronomy, Rutgers University, Piscataway, New Jersey 08854, USA*³*Center for Correlated Electron Systems, Institute for Basic Science (IBS), Seoul 08826, Republic of Korea*⁴*Department of Physics and Astronomy, Seoul National University, Seoul 08826, Republic of Korea*

(Received 13 February 2020; accepted 9 April 2020; published 18 May 2020; corrected 4 December 2020)

The Hall effect in SrRuO₃ thin films near the thickness limit for ferromagnetism shows an extra peak in addition to the ordinary and anomalous Hall effects. This extra peak has been attributed to a topological Hall effect due to two-dimensional skyrmions in the film around the coercive field; however, the sign of the anomalous Hall effect in SrRuO₃ can change as a function of saturation magnetization. Here we report Hall peaks in SrRuO₃ in which volumetric magnetometry measurements and magnetic force microscopy indicate that the peaks result from the superposition of two anomalous Hall channels with opposite sign. These channels likely form due to thickness variations in SrRuO₃, creating two spatially separated magnetic regions with different saturation magnetizations and coercive fields. The results are central to the development of strongly correlated materials for spintronics.

DOI: [10.1103/PhysRevMaterials.4.054414](https://doi.org/10.1103/PhysRevMaterials.4.054414)

I. INTRODUCTION

In the Hall effect a transverse electric field (E_x) is generated under an applied longitudinal current density (J_y). In conventional tensor notation, $E_x = \rho_{xy}J_y$, where ρ_{xy} is the Hall resistivity. In a ferromagnet, $\rho_{xy} = R_0H_z + R_sM_z$. The ordinary Hall effect (OHE) coefficient (R_0) is proportional to the out-of-plane applied magnetic field (H_z), it is caused by the Lorentz force, and its sign follows the sign of the charge carriers; the anomalous Hall effect (AHE) coefficient (R_s) is proportional to the out-of-plane component of magnetization (M_z). Recently, there have been reports of an additional peak in the Hall resistivity [illustrated in Fig. 1(a)] in ultrathin films of ferromagnetic SrRuO₃ [1–21]. This additional peak is sometimes attributed to a spin texture with net spin chirality [1–11,22], which results in electrons experiencing an effective magnetic field from the accumulation of a Berry phase in real space. This additional contribution to the Hall effect is called the topological Hall effect (THE) [23] [Fig. 1(b)]. A possible source of chirality is skyrmions in the SrRuO₃, which are topologically protected magnetic textures. Skyrmions can be stabilized through a competition between the ferromagnetic exchange and the Dzyaloshinskii-Moriya interaction (DMI) resulting from the combination of spin-orbit coupling and broken inversion symmetry. The source of spin-orbit coupling is either extrinsic from a heavy-metal oxide layer such as SrIrO₃ [1–3] or intrinsic to the SrRuO₃ [4–8]. The broken inversion symmetry arises from the interfaces between SrRuO₃ and adjacent layers. It is also possible that the DMI is sufficient

that domain walls around bubble domains have net chirality and therefore give a THE contribution [24].

Alternatively, the peak in the Hall effect could arise due to the superposition of two AHEs with different signs [13–21,25,26] [Fig. 1(c)]. The AHE in SrRuO₃ has a non-monotonic temperature and resistivity dependence which cannot be explained by scattering mechanisms alone [27–29]; instead, it is thought to also depend on the Berry curvature in k space [30–33]. This is an intrinsic mechanism for the Hall effect and should not be confused with the extrinsic accumulation of the Berry phase in real space by skyrmions. The anomalous Hall coefficient in SrRuO₃ is sensitively dependent on the band structure and magnetization [30,31], and is thus dependent on temperature (T) and thickness, as well as strain, disorder, and stoichiometry. Crucially, the AHE in SrRuO₃ undergoes a sign change as a function of saturation magnetization [13,34,35]. Therefore, if the SrRuO₃ is inhomogeneous, consisting of two magnetic regions with different coercive fields and saturation magnetizations giving opposite-sign AHEs, a peak will necessarily appear in the Hall effect.

In this paper, we show that the additional peak in the SrRuO₃ Hall effect is likely caused by the superposition of two opposite-sign AHEs from two magnetic regions with different saturation magnetizations. We argue that these two regions arise from single-unit-cell thickness variations in SrRuO₃ films that are close to the thickness limit for ferromagnetism. SrRuO₃ films between 4 and 5 pseudocubic unit cells (UCs) thick reproducibly display additional peaks in Hall effect measurements. Volumetric magnetometry shows two magnetic transition temperatures and two switching fields consistent with the Hall effect, and magnetic force microscopy (MFM) confirms that these two regions are spatially separated and magnetically nonuniform.

*jjr33@cam.ac.uk

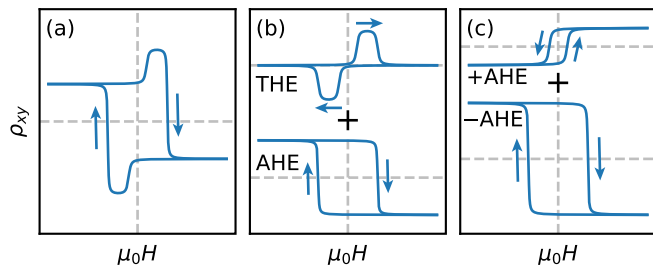


FIG. 1. (a) Illustrations of the peak structure in the Hall effect describing how the peaks may arise due to (b) the superposition of the AHE and THE, or (c) two AHE channels with different signs and coercive fields.

II. METHODS

SrRuO₃ films are grown by pulsed-laser deposition on TiO₂-terminated (001)-oriented SrTiO₃. The SrTiO₃ is held at 600 °C during deposition under a flow of 100-mTorr O₂, then cooled in 400-mTorr O₂ at $-5\text{ }^\circ\text{C min}^{-1}$. Laser pulses of 10 Hz with an energy density $\approx 2.5\text{ J cm}^{-2}$ give a growth rate of 1 UC ($c = 3.95\text{ \AA}$) per 10 seconds. SrRuO₃ grows initially layer-by-layer then transitions to step-flow growth after several UCs [36]. In the first layer, the substrate changes from *B*-site (TiO₂) to *A*-site (SrO) termination [37]. This can be considered as half-integer UC thicknesses of SrRuO₃, or as the first half UC being a continuation of the SrTiO₃ substrate; the latter definition is used here, as depicted in Fig. 2(c). The growth rate (and substrate terrace width) is high enough to reduce growth instabilities caused by the strain in SrRuO₃ [38], but low enough to allow for diffusion of adatoms across terraces [39]. TiO₂-terminated SrTiO₃ ensures uniform nucleation and growth of SrRuO₃ [40].

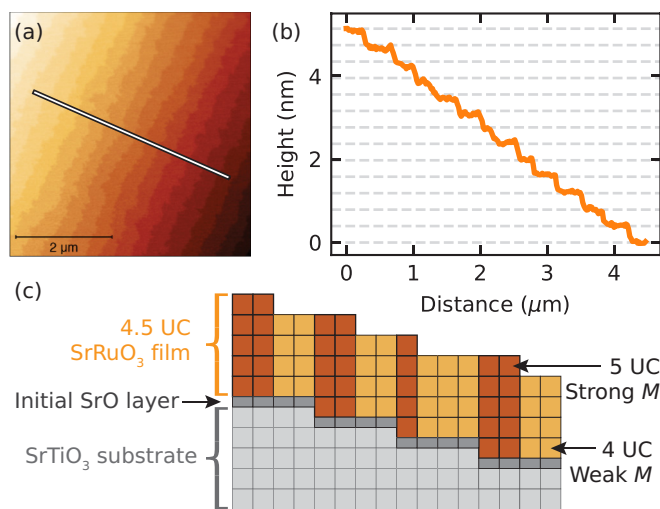


FIG. 2. (a) Plane-level AFM image of a 4.5-UC-thick SrRuO₃ film, showing a step-and-terrace structure typical of step-flow growth. (b) The corresponding height profile along the line drawn in (a); the horizontal dotted lines are separations of 1 UC ($c = 0.395\text{ nm}$, as measured in XRD on thicker films). (c) Illustration of thickness variations in the film.

The structural quality of films is assessed by x-ray diffraction (XRD), x-ray reflectivity (XRR), and atomic force microscopy (AFM). The growth rate is calibrated by fitting fringes in XRR [41] and XRD for thicker samples (see Supplemental Material [42]).

Volumetric magnetic properties are investigated using a superconducting quantum interference device with films loaded out-of-plane with respect to the applied magnetic field. To identify background signals, measurements were taken of the films, as-received substrates, and substrates which underwent the same growth and cleaning conditions as the film without any material deposited (see Supplemental Material [42,43]).

Transport measurements are made using unpatterned van der Pauw geometries. The transverse resistance data are antisymmetrized to separate the Hall effect from the longitudinal component of resistance (see Supplemental Material [42]).

Micromagnetic surface measurements are carried out using a cryogenic MFM with piezoresistive cantilevers, recorded in constant-height mode with the scanning plane 100 nm above the SrRuO₃ film surface. For further details see [44].

III. RESULTS AND DISCUSSION

SrRuO₃ films are epitaxial and fully strained to the SrTiO₃ substrate (see Supplemental Material [42]). Figure 2(a) shows an AFM image of a 4.5-UC-thick film with an atomically flat surface and a step-and-terrace structure. A line profile [Fig. 2(b)] shows the steps are 1 UC in height ($c = 3.95\text{ \AA}$), indicating a single surface termination in the SrRuO₃. Strain-induced growth instabilities in SrRuO₃ usually manifest as curvature at step edges.

Electronic transport of a 10-nm-thick SrRuO₃ film [Figs. 3(a) and 3(b)] shows a spontaneous Hall resistance ($R_{xy,s}$) attributed to the AHE, which changes sign from positive at high T to negative at low T . This unusual T dependence has been observed previously [31,35] and is related to the intrinsic nature of the AHE in SrRuO₃. We note that the apparent two magnetic switches seen in this case are likely caused by the rotation of the easy axis in SrRuO₃ away from the out-of-plane direction with increasing thickness, and not by two magnetic regions [45]. The spontaneous volume magnetization (M_s) of a film is used as a scaling parameter for the AHE, so the magnetization of the 10-nm film is measured versus T [Fig. 3(c)], showing only one transition at the Curie temperature ($T_C \approx 144\text{ K}$). The spontaneous Hall resistivity ($\rho_{xy,s}$) and conductivity (estimated as $\sigma_{xy,s} \approx -\rho_{xy,s}/\rho_{xx}^2$, where ρ_{xx} is the longitudinal resistivity) are plotted in Figs. 3(d) and 3(e). The Hall conductivity as a function of magnetization agrees well with literature values [31] despite differences in material properties. The anomalous Hall resistivity switches from positive at low M_s to negative at high M_s .

Hall measurements of a 4.5-UC-thick film shows additional peaks in R_{xy} , similar to those attributed to a THE. Figure 4(a) shows the T dependence of $R_{xy}(H)$, with peaks below 90 K; these data are fitted assuming the two-channel AHE model, and Fig. 4(b) is the same data at only 10 K. The data are well reproduced by these two AHEs [Fig. 4(c)]. The spontaneous anomalous Hall resistances of the two channels extracted from the fit are shown as a function of T in Fig. 4(f). The T dependence of the two AHE channels can be compared

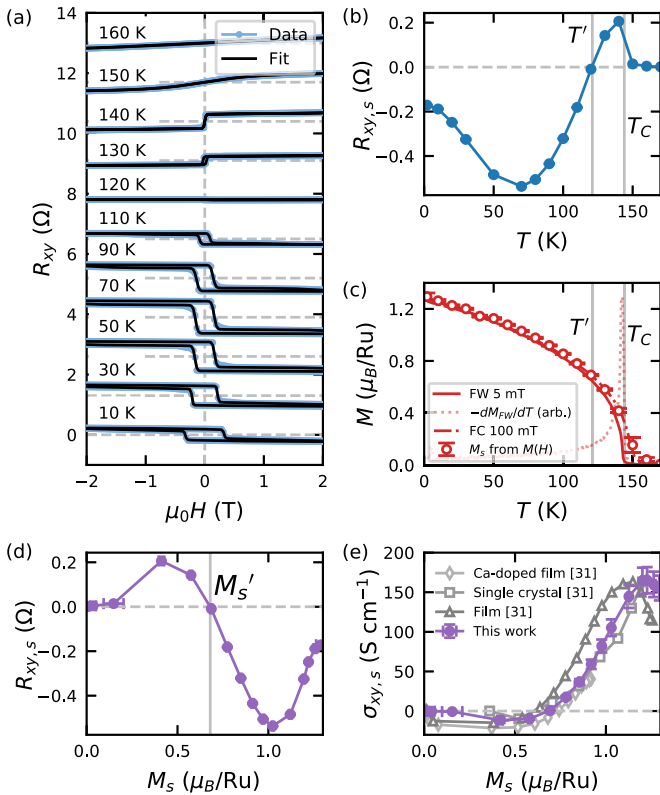


FIG. 3. Transport and magnetometry of a 10-nm-thick film. (a) $R_{xy}(H)$ at different T . The OHE is removed by a linear fitting at high field (5–6 T). (b) The spontaneous anomalous Hall effect extracted from (a) as a function of temperature. This is nonmonotonic with a sign change at $T' \approx 121$ K. (c) Magnetization as a function of temperature. Field-cooling and field-warming curves have substrate curves subtracted and are shifted vertically so $M(170) = 0$; the dotted curve shows the derivative of the 5-mT field-warming curve with arbitrary units to highlight the magnetic transition. Points from $M(H)$ curves are spontaneous magnetization taken as average moment under 1 T for saturated quadrants. There is no magnetic transition evident at the AHE sign change. (d) Spontaneous anomalous Hall resistivity of the SrRuO_3 as a function of spontaneous magnetization. The anomalous Hall effect is positive for small M_s and negative for large M_s , switching at $M'_s \approx 0.7 \mu_B/\text{Ru}$. (e) Spontaneous anomalous Hall conductivity as a function of spontaneous magnetization, compared to previous literature values [31].

to that of the thicker film [Fig. 3(b)]: a similar T dependence is seen but suppressed to lower T slightly in AHE_2 , and suppressed significantly in AHE_1 .

An $M(H)$ loop at 10 K is shown in Fig. 4(d) (for the full temperature range see the Supplemental Material [42]). This is fitted using the same function as for the anomalous Hall effect, where only the scalings of the two components are varied as free parameters; these two components are shown in Fig. 4(e). There are two clear switches in the magnetometry which correspond to the two switches in Hall effect, and the smaller magnetic switch gives a positive-AHE component, while the larger switch gives a negative AHE, as expected.

The magnetization versus temperature is shown in Fig. 4(g); there appear to be two separate magnetic transitions which is most obvious in the remanence curve (saturating with 7 T and warming in a 5-mT field; solid curve) and

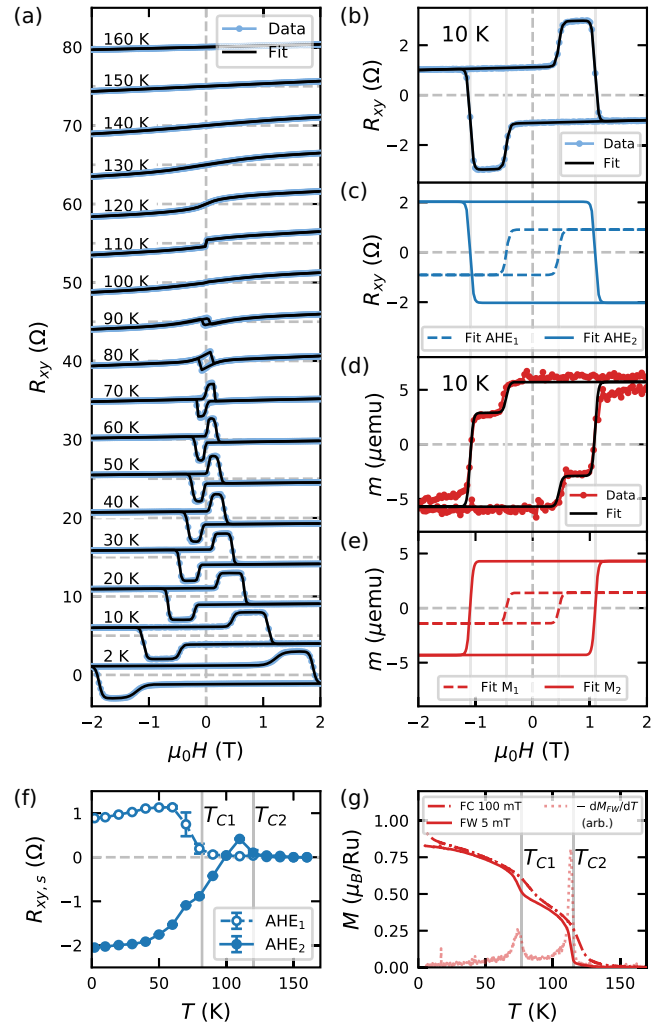


FIG. 4. Transport and magnetometry of a 4.5-UC-thick SrRuO_3 film. (a) $R_{xy}(H)$ at different T . The data (blue points) are fitted to a function of two sigmoids as an approximation of two AHEs (black line). (b) $R_{xy}(H)$ of the film at 10 K; the black line is the two-AHE fit. (c) The two fit components from (b). (d) Moment (m) versus H of the film at 10 K, showing two switches at the same coercive fields as in the Hall resistance. For the fit, the widths and coercive fields from (b) and (c) are fixed, and the scalings are fit parameters. (e) The two fit components from (d). (f) T dependence of the spontaneous anomalous Hall resistance of the two channels, defined as the mean and standard deviation of anomalous Hall resistance in the 0–100 mT range of the saturated quadrant of an individual fit component. (g) T dependence of the magnetization in field cooling (FC) in 100 mT, and field warming (FW) in 5 mT after saturating at 7 T. Data have substrate curves subtracted and are shifted vertically so $M(170) = 0$. The dotted curve shows the derivative of the 5-mT field-warming curve with arbitrary units to highlight the two magnetic transitions.

its derivative (dotted curve; arbitrary units and flipped for clarity), which show two transitions at $T_{C1} \approx 77$ K and $T_{C2} \approx 115$ K, labeled on the graph with solid gray lines. These two transition temperatures are also plotted in Fig. 4(f) and agree with the appearance of the spontaneous components of each AHE channel, so we attribute these transitions to the Curie temperatures for the two magnetic regions. It is likely

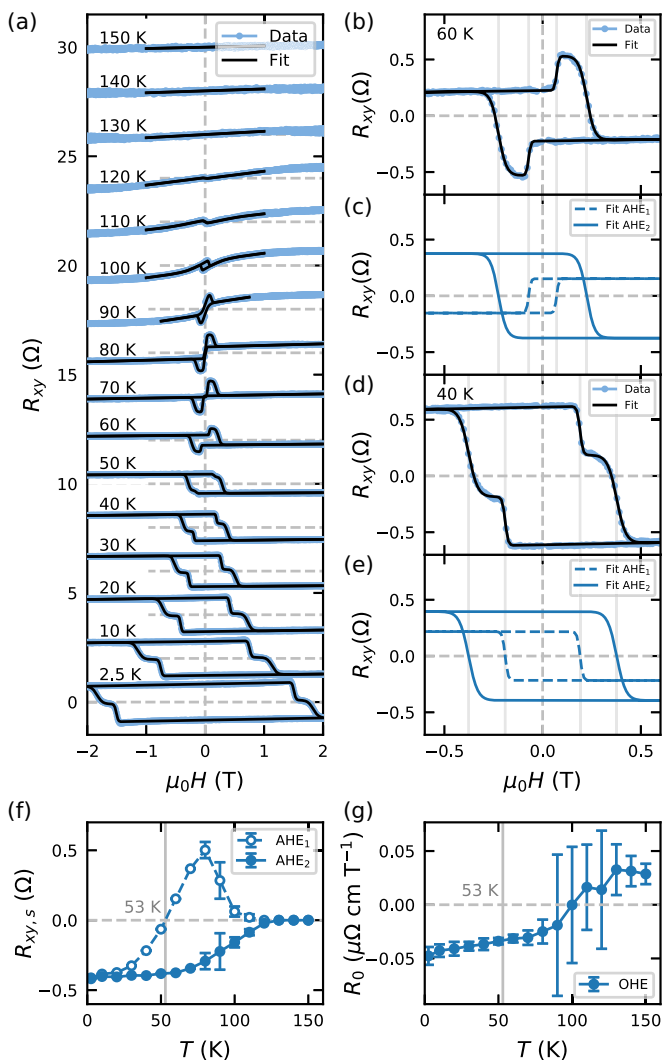


FIG. 5. Transport measurements of a nominally 4.0-UC-thick SrRuO₃ film. (a) T dependence of $R_{xy}(H)$, showing a transition from the usual “peak” shape below T_C to a “step” shape at 50 K and below. (b) $R_{xy}(H)$ at 60 K showing the usual “peak” shape, with the fitting shown in black. (c) The two components of the fit at 60 K: one positive and one negative AHE. (d) $R_{xy}(H)$ at 40 K showing the “step” shape, with the fitting shown in black. (e) The two components of the fit at 40 K: two negative AHEs. (f) T dependence of the two AHE components. One component experiences a sign change near 53 K, where the anomalous Hall signal changes from steplike at low T to peaklike at high T . (g) T dependence of the OHE, found from a linear fit at 2–3 T; the error is the difference between the OHE estimated by high-field and low-field fits. The error becomes very large above 90 K, where it becomes difficult to separate the broad paramagnetic AHE from the OHE. The OHE does not change sign near 53 K.

that the 4-UC regions correspond to the lower T_C , lower H_c , and positive AHE, while the 5-UC regions correspond to the higher T_C , higher H_c , and negative AHE (at low T).

A SrRuO₃ film prepared in a different system and measured sooner after deposition also shows two switches in $R_{xy}(H)$ [Fig. 5(a)], $R_{xy}(H)$ [Fig. 5(f)], $M(H)$, and $M(T)$ (see Supplemental Material [42]). However, the Hall effect transitions from a peaklike structure at high T [one low-

M_s positive-AHE region, one high- M_s negative-AHE region; Figs. 5(b) and 5(c)] to a steplike structure at low T [two high- M_s negative-AHE regions; Figs. 5(d) and 5(e)]. This steplike structure is consistent with two AHEs. To explain this in terms of the THE, the OHE or spin polarization of the SrRuO₃ would change sign at ≈ 53 K. An OHE sign change at this T is not observed here [Fig. 5(g)], but we note that though generally assumed to be constant below T_C , the temperature-dependent spin polarization of SrRuO₃ is not well characterized theoretically or experimentally. An alternative explanation might be that the THE peak is shifting to higher fields above the coercive field of SrRuO₃. This is, however, unlikely since an intermediate peak plus step shape is expected in this case.

MFM images show stripe domains in the SrRuO₃ films consisting of two regions with different H_c and magnetic strengths. Figures 6(a)–6(e) are MFM images at 10 K, 0.1 T after saturating at negative field and sequentially applying different fields, which are also shown on the $R_{xy}(H)$ loop in Fig. 6(f). Following the increasing field, at 0.2 T the film is still negatively magnetized and stripe contrast is present as thinner regions have a lower M_s ; at 0.4 T, weaker regions (yellow-green) are switching; at 0.9 T, weaker regions are now positively magnetized (light blue)—this switch corresponds to H_{c1} for the positive-AHE component (AHE₁); at 1.3 T, stronger magnetic regions (red) begin to switch (blue); at 1.6 T, all strong regions have switched to positive magnetization (blue)—this corresponds to H_{c2} for the negative-AHE component (AHE₂). The stripe contrast remains even at high field due to the difference in M_s between the two regions.

The root mean square (RMS) deviation of the MFM signal is also plotted in Fig. 6(f) (green squares). This quantifies the magnetic inhomogeneity in the film; this peak in RMS signal matches well with the peak in the Hall effect.

Figure 6(g) shows the change in MFM signal through the first switch, and Fig. 6(h) through the second switch; each switch corresponds to one set of stripes changing magnetization. The combination of these two images is shown in Fig. 6(i), the lack of overlap demonstrating that the two switches correspond to two spatially separated magnetic regions. These data are consistent with the picture that 1-UC thickness variations across terrace steps create two magnetic regions with different M_s , which results in two AHE channels with different signs, and due to their differing H_c , a peak appears in the Hall effect.

IV. CONCLUSION

The anomalous Hall coefficient in SrRuO₃ depends strongly on the band structure and magnetization, and can switch sign with parameters that affect these, such as temperature, film thickness, or disorder. In a SrRuO₃ thin film, if there are two magnetic regions with different coercive fields and signs of the AHE, then peaks will appear in Hall effect measurements. Here, 4 to 5 UC thick SrRuO₃ films show peaks in the Hall effect; similar peaks have been observed previously and are sometimes attributed to a THE caused by magnetic skyrmions. SrRuO₃ films in this work show two spatially separated magnetic regions with different T_C , M_s , and H_c values. The stripe pattern of these two regions indicates they likely result from step-flow growth giving single-unit-cell

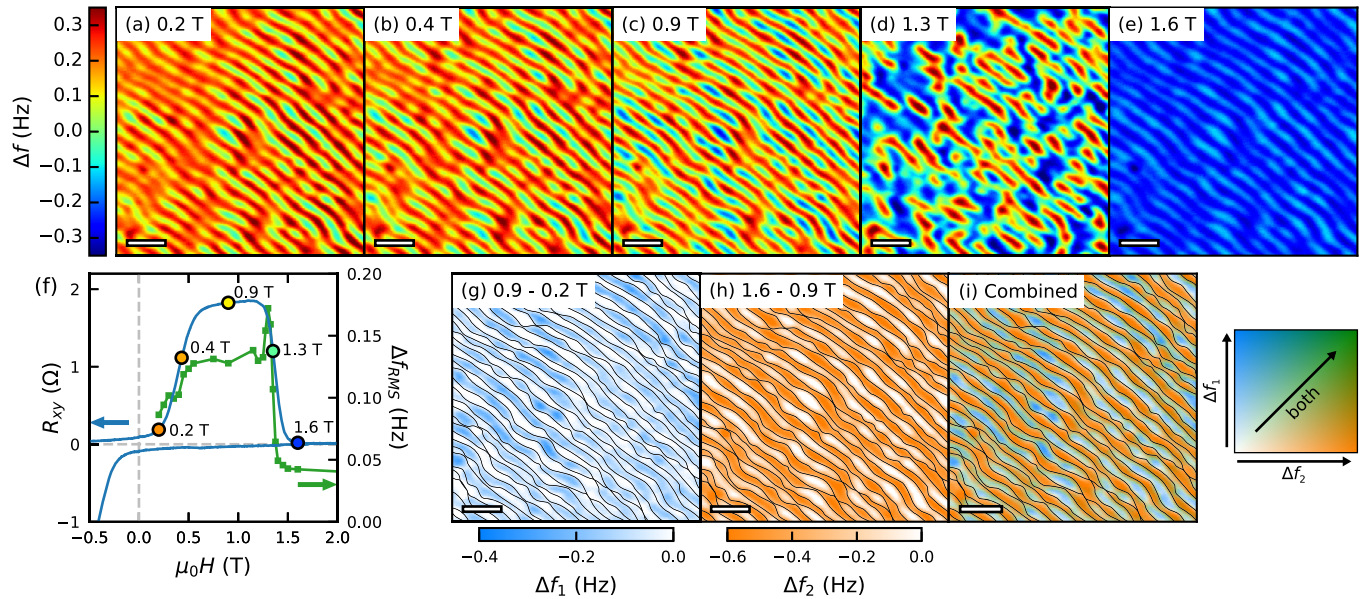


FIG. 6. MFM images at 10 K, 0.1 T after applying different fields. Scale bars are $1 \mu\text{m}$. Δf , the change in resonant frequency, is proportional to out-of-plane stray field gradient. The sign of Δf is opposite to the sign of magnetization. Panels (a)–(e) show the progression of the magnetic structure of the film through the two transitions. Red/yellow is negatively magnetized, blue/cyan is positively magnetized. Panel (f) shows the anomalous Hall resistance (blue line) of the film as a function of field, with points labeled where the presented MFM images were measured. The RMS deviation of the MFM signal (green squares) shows a peak in inhomogeneity corresponding to the peak in the Hall effect. (g) The change in MFM signal through the first transition, showing only one set of stripes switching. Black lines are added as a guide to the eye. (h) The change in MFM signal through the second transition, showing the other set of stripes switching. The same black lines are a guide to the eye. (i) The images from (g) and (h) combined additively. The MFM signal either changes in the first transition or the second rather than both, meaning there are two spatially magnetic regions with two different coercive fields.

thickness variations in the film across terrace steps. These two magnetic regions can explain the peaks in the Hall effect by the superposition of two AHEs with different signs. Additionally, a film showed a smooth transition from peaklike to steplike Hall effect, which is not easily explained by a THE.

These data do not exclude the existence of a THE; however, we show that the observation of a peak in the Hall effect does not give unambiguous evidence for a THE caused by magnetic skyrmions, particularly in the case where the magnetic structure of the SrRuO_3 film is inhomogeneously modified.

ACKNOWLEDGMENTS

This work is supported by the EPSRC through the Core-to-Core International Network ‘‘Oxide Superspin’’ (EP/P026311/1) and the Doctoral Training Partnership Grant (EP/N509620/1). Additional support is provided by the Office of Basic Energy Sciences, Division of Materials Sciences and Engineering, US Department of Energy, under Award No. DE-SC0018153, and the Research Center Program of IBS (Institute for Basic Science) in Korea (IBS-R009-D1).

- [1] J. Matsuno, N. Ogawa, K. Yasuda, F. Kagawa, W. Koshibae, N. Nagaosa, Y. Tokura, and M. Kawasaki, Interface-driven topological Hall effect in SrRuO_3 - SrIrO_3 bilayer, *Sci. Adv.* **2**, e1600304 (2016).
- [2] Y. Ohuchi, J. Matsuno, N. Ogawa, Y. Kozuka, M. Uchida, Y. Tokura, and M. Kawasaki, Electric-field control of anomalous and topological Hall effects in oxide bilayer thin films, *Nat. Commun.* **9**, 213 (2018).
- [3] K.-Y. Meng, A. S. Ahmed, M. Baćani, A.-O. Mandru, X. Zhao, N. Bagnés, B. D. Esser, J. Flores, D. W. McComb, H. J. Hug, and F. Yang, Observation of nanoscale skyrmions in $\text{SrIrO}_3/\text{SrRuO}_3$ bilayers, *Nano Lett.* **19**, 3169 (2019).
- [4] B. Sohn, B. Kim, S. Y. Park, H. Y. Choi, J. Y. Moon, T. Choi, Y. J. Choi, T. W. Noh, H. Zhou, S. H. Chang, J. H. Han, and C. Kim, Emergence of robust 2D skyrmions in SrRuO_3 ultrathin film without the capping layer, [arXiv:1810.01615](https://arxiv.org/abs/1810.01615).
- [5] Y. Gu, Y.-W. Wei, K. Xu, H. Zhang, F. Wang, F. Li, M. S. Saleem, C.-Z. Chang, J. Sun, C. Song, J. Feng, X. Zhong, W. Liu, Z. Zhang, J. Zhu, and F. Pan, Interfacial oxygen-octahedral-tilting-driven electrically tunable topological Hall effect in ultrathin SrRuO_3 films, *J. Phys. D* **52**, 404001 (2019).
- [6] Q. Qin, L. Liu, W. Lin, X. Shu, Q. Xie, Z. Lim, C. Li, S. He, G. M. Chow, and J. Chen, Emergence of topological Hall effect in a SrRuO_3 single layer, *Adv. Mater.* **31**, 1807008 (2019).
- [7] B. Sohn, B. Kim, J. W. Choi, S. H. Chang, J. H. Han, and C. Kim, Hump-like structure in Hall signal from ultra-thin SrRuO_3 films without inhomogeneous anomalous Hall effect, *Curr. Appl. Phys.* **20**, 186 (2020).
- [8] P. Zhang, A. Das, E. Barts, M. Azhar, L. Si, K. Held, M. Mostovoy, and T. Banerjee, Robust skyrmion-bubble textures in SrRuO_3 thin films stabilized by magnetic anisotropy, [arXiv:2001.07039](https://arxiv.org/abs/2001.07039).

- [9] L. Wang, Q. Feng, Y. Kim, R. Kim, K. H. Lee, S. D. Pollard, Y. J. Shin, H. Zhou, W. Peng, D. Lee, W. Meng, H. Yang, J. H. Han, M. Kim, Q. Lu, and T. W. Noh, Ferroelectrically tunable magnetic skyrmions in ultrathin oxide heterostructures, *Nat. Mater.* **17**, 1087 (2018).
- [10] W. Wang, M. W. Daniels, Z. Liao, Y. Zhao, J. Wang, G. Koster, G. Rijnders, C.-Z. Chang, D. Xiao, and W. Wu, Spin chirality fluctuation in two-dimensional ferromagnets with perpendicular magnetic anisotropy, *Nat. Mater.* **18**, 1054 (2019).
- [11] Z. Li, S. Shen, Z. Tian, K. Hwangbo, M. Wang, Y. Wang, F. M. Bartram, L. He, Y. Lyu, Y. Dong, G. Wan, H. Li, N. Lu, J. Zang, H. Zhou, E. Arenholz, Q. He, L. Yang, W. Luo, and P. Yu, Reversible manipulation of the magnetic state in SrRuO₃ through electric-field controlled proton evolution, *Nat. Commun.* **11**, 184 (2020).
- [12] Y. Gu, C. Song, Q. Zhang, F. Li, H. Tan, K. Xu, J. Li, M. S. Saleem, M. U. Fayaz, J. Peng, F.-X. Hu, L. Gu, W. Liu, Z. Zhang, and F. Pan, Interfacial control of ferromagnetism in ultrathin SrRuO₃ films sandwiched between ferroelectric BaTiO₃ layers, *ACS Appl. Mater. Interfaces* **12**, 6707 (2020).
- [13] D. J. Groenendijk, C. Autieri, T. C. van Thiel, W. Brzezicki, N. Gauquelin, P. Barone, K. H. W. v. d. Bos, S. van Aert, J. Verbeeck, A. Filippetti, S. Picozzi, M. Cuoco, and A. D. Caviglia, Berry phase engineering at oxide interfaces, [arXiv:1810.05619](https://arxiv.org/abs/1810.05619).
- [14] D. Kan, T. Moriyama, K. Kobayashi, and Y. Shimakawa, Alternative to the topological interpretation of the transverse resistivity anomalies in SrRuO₃, *Phys. Rev. B* **98**, 180408(R) (2018).
- [15] G. Malsch, D. Ivaneyko, P. Milde, L. Wysocki, L. Yang, P. H. M. van Loosdrecht, I. Lindfors-Vrejoiu, and L. M. Eng, Correlating the nanoscale structural, magnetic and magneto-transport properties in SrRuO₃-based perovskite oxide ultra-thin films, *ACS Appl. Nano Mater.* **3**, 1182 (2020).
- [16] Z. Y. Ren, Z. Yuan, L. F. Wang, F. Shao, P. F. Liu, J. Teng, K. K. Meng, X. G. Xu, J. Miao, and Y. Jiang, Nonvolatile ferroelectric field control of the anomalous Hall effect in BiFeO₃/SrRuO₃ bilayer, [arXiv:1910.02588](https://arxiv.org/abs/1910.02588).
- [17] L. Wang, Q. Feng, H. G. Lee, E. K. Ko, Q. Lu, and T. W. Noh, Controllable thickness inhomogeneity and Berry curvature engineering of anomalous Hall effect in SrRuO₃ ultrathin films, *Nano Lett.* **20**, 2468 (2020).
- [18] L. Wu, F. Wen, Y. Fu, J. H. Wilson, X. Liu, Y. Zhang, D. M. Vasiukov, M. S. Kareev, J. H. Pixley, and J. Chakhalian, Berry phase manipulation in ultrathin SrRuO₃ films, [arXiv:1907.07579](https://arxiv.org/abs/1907.07579).
- [19] M. Ziese, L. Jin, and I. Lindfors-Vrejoiu, Unconventional anomalous Hall effect driven by oxygen-octahedra-tailoring of the SrRuO₃ structure, *J. Phys.: Mater.* **2**, 034008 (2019).
- [20] P.-C. Wu, H. Song, Y. Yuan, B. Feng, Y. Ikuhara, R. Huang, P. Yu, C.-G. Duan, and Y.-H. Chu, Thickness dependence of transport behaviors in SrRuO₃/SrTiO₃ superlattices, *Phys. Rev. Mater.* **4**, 014401 (2020).
- [21] D. Kan, T. Moriyama, and Y. Shimakawa, Field-sweep-rate and time dependence of transverse resistivity anomalies in ultrathin SrRuO₃ films, *Phys. Rev. B* **101**, 014448 (2020).
- [22] B. M. Ludbrook, G. Dubuis, A.-H. Puichaud, B. J. Ruck, and S. Granville, Nucleation and annihilation of skyrmions in Mn₂CoAl observed through the topological Hall effect, *Sci. Rep.* **7**, 1 (2017).
- [23] P. Bruno, V. K. Dugaev, and M. Taillefumier, Topological Hall Effect and Berry Phase in Magnetic Nanostructures, *Phys. Rev. Lett.* **93**, 096806 (2004).
- [24] J. Jiang, D. Xiao, F. Wang, J.-H. Shin, D. Andreoli, J. Zhang, R. Xiao, Y.-F. Zhao, M. Kayyalha, L. Zhang, K. Wang, J. Zang, C. Liu, N. Samarth, M. H. W. Chan, and C.-Z. Chang, Concurrence of quantum anomalous Hall and topological Hall effects in magnetic topological insulator sandwich heterostructures, *Nat. Mater.* (2020).
- [25] A. Gerber, Interpretation of experimental evidence of the topological Hall effect, *Phys. Rev. B* **98**, 214440 (2018).
- [26] L. Wu and Y. Zhang, Artificial topological Hall effect induced by intrinsic thickness non-uniformity in ultrathin SrRuO₃ films, [arXiv:1812.09847](https://arxiv.org/abs/1812.09847).
- [27] L. Berger, Side-jump mechanism for the Hall effect of ferromagnets, *Phys. Rev. B* **2**, 4559 (1970).
- [28] J. Smit, The spontaneous Hall effect in ferromagnetics. I, *Physica* **21**, 877 (1955).
- [29] J. Smit, The spontaneous Hall effect in ferromagnetics. II, *Physica* **24**, 39 (1958).
- [30] M. Onoda and N. Nagaosa, Topological nature of anomalous Hall effect in ferromagnets, *J. Phys. Soc. Jpn.* **71**, 19 (2002).
- [31] Z. Fang, N. Nagaosa, K. S. Takahashi, A. Asamitsu, R. Mathieu, T. Ogasawara, H. Yamada, M. Kawasaki, Y. Tokura, and K. Terakura, The anomalous Hall effect and magnetic monopoles in momentum space, *Science* **302**, 92 (2003).
- [32] T. Jungwirth, Q. Niu, and A. H. MacDonald, Anomalous Hall Effect in Ferromagnetic Semiconductors, *Phys. Rev. Lett.* **88**, 207208 (2002).
- [33] N. Haham, Y. Shperber, M. Schultz, N. Naftalis, E. Shimshoni, J. W. Reiner, and L. Klein, Scaling of the anomalous Hall effect in SrRuO₃, *Phys. Rev. B* **84**, 174439 (2011).
- [34] R. Mathieu, A. Asamitsu, H. Yamada, K. S. Takahashi, M. Kawasaki, Z. Fang, N. Nagaosa, and Y. Tokura, Scaling of the Anomalous Hall Effect in Sr_{1-x}Ca_xRuO₃, *Phys. Rev. Lett.* **93**, 016602 (2004).
- [35] L. Klein, J. R. Reiner, T. H. Geballe, M. R. Beasley, and A. Kapitulnik, Extraordinary Hall effect in SrRuO₃, *Phys. Rev. B* **61**, R7842 (2000).
- [36] J. Choi, C. B. Eom, G. Rijnders, H. Rogalla, and D. H. A. Blank, Growth mode transition from layer by layer to step flow during the growth of heteroepitaxial SrRuO₃ on (001) SrTiO₃, *Appl. Phys. Lett.* **79**, 1447 (2001).
- [37] G. Rijnders, D. H. A. Blank, J. Choi, and C.-B. Eom, Enhanced surface diffusion through termination conversion during epitaxial SrRuO₃ growth, *Appl. Phys. Lett.* **84**, 505 (2004).
- [38] D. Estève, T. Maroutian, V. Pillard, and P. Lecoeur, Step velocity tuning of SrRuO₃ step flow growth on SrTiO₃, *Phys. Rev. B* **83**, 193401 (2011).
- [39] R. A. Rao, Q. Gan, and C. B. Eom, Growth mechanisms of epitaxial metallic oxide SrRuO₃ thin films studied by scanning tunneling microscopy, *Appl. Phys. Lett.* **71**, 1171 (1997).

- [40] R. Bachelet, F. Sánchez, J. Santiso, C. Munuera, C. Ocal, and J. Fontcuberta, Self-assembly of SrTiO₃ (001) chemical-terminations: A route for oxide-nanostructure fabrication by selective growth, *Chem. Mater.* **21**, 2494 (2009).
- [41] M. Björck and G. Andersson, GenX: An extensible x-ray reflectivity refinement program utilizing differential evolution, *J. Appl. Crystallogr.* **40**, 1174 (2007).
- [42] See Supplemental Material at <http://link.aps.org/supplemental/10.1103/PhysRevMaterials.4.054414> for additional details and characterization of samples.
- [43] M. Khalid, A. Setzer, M. Ziese, P. Esquinazi, D. Spemann, A. Pöpl, and E. Goering, Ubiquity of ferromagnetic signals in common diamagnetic oxide crystals, *Phys. Rev. B* **81**, 214414 (2010).
- [44] P. M. Sass, W. Ge, J. Yan, D. Obeysekera, J. J. Yang, and W. Wu, Magnetic imaging of antiferromagnetic domain walls, *Nano Lett.* **20**, 2609 (2020).
- [45] M. Schultz, S. Levy, J. W. Reiner, and L. Klein, Magnetic and transport properties of epitaxial films of SrRuO₃ in the ultrathin limit, *Phys. Rev. B* **79**, 125444 (2009).

Correction: The caption to Figure 2 contained a typographical error and has been fixed.